Bioelectrochemistry 142 (2021) 107932

Contents lists available at ScienceDirect

Bioelectrochemistry

journal homepage: www.elsevier.com/locate/bioelechem

Contrast-enhanced ultrasound for evaluation of tumor perfusion and outcome following treatment in a murine melanoma model

Maja Brloznik [a], Nina Boc [b], Maja Cemazar [b,e], Masa Bosnjak [b], Monika Savarin [b], Natasa Kejzar [c], Gregor Sersa [b,d], Darja Pavlin [a,*], Simona Kranjc Brezar [b,f,*]

[a] Small Animal Clinic, Veterinary Faculty, University of Ljubljana, Gerbiceva 60, Ljubljana, Slovenia
[b] Institute of Oncology Ljubljana, Zaloska 2, Ljubljana, Slovenia
[c] Institute for Biostatistics and Medical Informatics, Faculty of Medicine, University of Ljubljana, Vrazov trg 2, Ljubljana, Slovenia
[d] Faculty of Health Sciences, University of Ljubljana, Zdravstvena pot 5, Ljubljana, Slovenia
[e] Faculty of Health Sciences, University of Primorska, Polje 42, Izola, Slovenia
[f] Faculty of Medicine, University of Ljubljana, Vrazov trg 2, Ljubljana, Slovenia

ARTICLE INFO

Article history:
Received 1 November 2020
Received in revised form 10 August 2021
Accepted 13 August 2021
Available online 18 August 2021

Keywords:
Murine melanoma B16F10
Gene electrotransfer
Melanoma cell adhesion molecule
Irradiation
Antivascular effects
Contrast-enhanced harmonic ultrasound

ABSTRACT

Due to a lack of data on predictors of electroporation-based treatment outcomes, we investigated the potential predictive role of contrast-enhanced harmonic ultrasound (CEUS) in mice B16F10 melanoma treated by gene electrotransfer (GET) to silence melanoma cell adhesion molecule (MCAM) and radiotherapy, which has not been evaluated yet. CEUS evaluation was verified by tumor histological analysis. Mice bearing subcutaneous tumors were treated with GET to silence MCAM, irradiation or the combination of GET to silence MCAM and irradiation (combined treatment). CEUS of the tumors used to evaluate tumor perfusion was performed before and up to 10 days after the beginning of the experiment, and the CEUS results were compared with tumor growth and the number of blood vessels analyzed in the histological tumor sections. CEUS revealed a decrease in tumor perfusion in the combined therapy groups compared with the control groups and correlated with tumor histological analyses, which showed a decreased vascular density. In this study a trend of inverse correlation was observed between tumor perfusion and treatment efficacy. The greater the perfusion of the tumor, the shorter the expected doubling time. Furthermore, decreased perfusion showed a trend to correlate with higher antitumor efficacy. Thus, CEUS could be used to predict tumoral vascular density and treatment effectiveness.

1. Introduction

The tumor vasculature is an attractive target for cancer therapy. A single vessel facilitates the survival of multiple tumor cells and provides the main route for metastatic spread [1]. Therefore, tumor vessel density and certain tumor perfusion aspects have been intensively investigated as possible predictors of tumor behavior and treatment outcome. A method to detect tissue perfusion at the capillary level is contrast-enhanced harmonic ultrasound (CEUS). In preclinical studies, it was shown to be an accurate predictor of tumor vascularization compared with histological results [2–4], and it correlated with advanced diagnostic imaging methods [5]. Furthermore, CEUS proved to be valuable in assessing the tumor response to treatment and as a possible means to guide the drug dosages [3–5]. In human and canine clinical studies, CEUS was able to determine microvessel density [6–9]. In humans, it has been proven to be a useful tool to evaluate the efficacy of anti-angiogenic treatments [10–13]. CEUS parameters measure tissue perfusion at the capillary level: some of them describe blood volume and others blood flow rate. Perfusion parameters are influenced by cardiac, vascular, microcirculatory and other factors [13].

Gene electrotransfer (GET) is a physical method of plasmid DNA delivery into cells, enabling the entry of large molecules by application of short high-voltage electric pulses that induce cell membrane permeabilization [14–16]. Melanoma cell adhesion molecule (MCAM) or CD146 is a multifunctional transmembrane glycoprotein, which is overexpressed in melanoma and is involved in melanoma development and progression, the latter including invasiveness, metastatic potential, and angiogenesis. Therefore, the silencing of MCAM, using plasmid DNA encoding shRNA

* Corresponding authors at: Small animal clinic, Veterinary Faculty, University of Ljubljana, Gerbiceva 60, Ljubljana (D. Pavlin); Institute of Oncology Ljubljana, Zaloska 2, Ljubljana, Slovenia (S. Kranjc Brezar).
E-mail addresses: darja.pavlin@vf.uni-lj.si (D. Pavlin), skranjc@onko-i.si (S. Kranjc Brezar).

https://doi.org/10.1016/j.bioelechem.2021.107932
1567-5394/

against MCAM, is a potential target for the gene therapy of melanoma [17–19].

Vascular targeted therapies aim at normalizing the tumor vasculature and therefore promote radiosensitizing effects because they facilitate increased oxygenation of the remaining tumor tissue [1,21–23]. GET of plasmid DNA exhibits a radiosensitizing effect in murine tumors [19–23], and studies have shown that both therapeutic and control plasmid DNA devoid of therapeutic genes have antitumor action [19,24–26].

Despite clinical effectiveness of electroporation-based therapies there is still a lack of data on predictors of treatment outcome. Thus, this study aimed to compare the results of CEUS with histological analysis of the tumor vascular density and evaluate them as possible predictive factors for the therapeutic outcome in an experimental model of radioresistant murine melanoma B16F10 treated with irradiation and gene electrotransfer (GET) of plasmid DNA encoding shRNA against MCAM.

2. Materials and methods

2.1. Animals

Female C57Bl/6JOlaHsd mice (Envigo RMS SrL, San Pietro al Natisone, Italy), 7 weeks old, weighing 18–20 g, were housed under specific pathogen-free conditions at a temperature of 20–24 °C and with a relative humidity of 55 ± 10%, a 12-hour light/dark cycle, and food and water provided ad libitum. All the procedures were performed according to the guidelines for animal experiments of the EU directive (2010/63/EU). Regulatory approval was issued by the Veterinary Administration of the Ministry of Agriculture and the Environment of the Republic of Slovenia (No. U34401-1/2015/38).

2.2. Tumors

The subcutaneous tumors were induced on the back of the mice by the subcutaneous injection of 100 μl of B16F10 cell suspension containing one million cells (American Type Culture Collection, Manassas, VA, USA). The cells were cultured in advanced minimum essential medium (AMEM) supplemented with 5% fetal bovine serum (FBS), 10 mM/l L-glutamine GlutaMAX (all Gibco, Fisher Scientific, Waltham, MA, USA), 100 U/ml of penicillin (Grünenthal, Aachen, Germany) and 50 mg/ml of gentamicin (Krka, Novo mesto, Slovenia) in a 5% CO_2 humidified incubator at 37 °C. At 80% confluence, trypsinization was performed with 0.25% trypsin/EDTA in Hank's buffer and the cells were then washed with AMEM with FBS and collected by centrifugation. The cells were routinely checked for the presence of *Mycoplasma sp* (MycoAlertTM PLUS Mycoplasma Detection Kit; Pharma & Biotech, Lonza, Basel, Switzerland).

2.3. Experimental protocol

The tumors were allowed to reach a volume of approximately 40 mm^3, which corresponds to a diameter of approximately 6 × 6 × 2 mm (day 0). The tumors were measured every second day with a Vernier-caliper, and the tumor volume was calculated from the measured perpendicular diameters ($V = a \times b \times c \times \pi/6$).

The mice were randomly divided into twelve groups, each containing nine or ten mice. The procedures performed in the treatment groups are presented in Table 1.

Irradiation was delivered by a Darpac 2000 X-ray unit (Gulmay Medical Ltd, Surrey, UK) operating at 220 kV, 10 mA, with 1.8-mm aluminum filtration. Possible acute skin reactions in the irradiated field were monitored as described previously [21,27,28].

Electric pulses were generated by an electric pulse generator ELECTRO CELL B10 HVLV (Betatech, L'Union, France) and delivered through two parallel stainless steel electrodes 6–7 mm apart, depending on the tumor volume. After the delivery of four pulses, the electrodes were turned for 90° to deliver four additional pulses. The selection of voltage, duration and frequency of EP was chosen based on previous studies [14,15].

For EP and CEUS, the mice were anesthetized using inhalation anesthesia with isoflurane (2% v/v), and the heating pad was used to prevent hypothermia. For CEUS examinations, the tumors were fixed in a plastic holder to improve tumor display and for more stable probe holding.

CEUS examinations were performed in three to seven animals of each group on days 0, 1, 2, 5, 6, 7 and/or 10. On days 0, 1 and 2, CEUS examinations were performed before other procedures. The schedule of the experiment is shown in Scheme 1. The mice used for tumor histology were humanely sacrificed on day 6. Mice were humanely sacrificed due to disease burden when tumor diameter was larger than 12 mm. Most of the statistical analyses were performed until day 7; however, from day 6, the sample of mice is biased toward mice with a lower disease burden.

The contrast agent Sonovue (Bracco, Milan, Italy), ultrasonographic machine M9 (Mindray, Shenzhen, China) and linear probe (L3-13.5; Mindray, Shenzhen, China) with a frequency of 3 to 13.5 MHz and harmonic ultraband nonlinear contrast display at a low mechanical index were used. The clinical guidelines for CEUS to quantify tumor perfusion were followed [29–31]. After applying 50 μl of the topical anesthetic Alcaine ophthalmic solution (Alcon, Basel, Switzerland) to the mice cornea, 0.1 ml of contrast agent was administered to the retroorbital sinus [32]. From the time of contrast application, a 90-second-long recording was made. Each tumor was carefully delineated, and 6 to 8 ellipsoid regions of interest (ROIs) were drawn to cover the whole area of the tumor (Supplementary Figure S1). For the whole tumor and ROIs, the perfusion curve or time-intensity curve, presenting the signal intensity, was analyzed using an ultrasound (US) system with built-in software.

Animal weight was monitored as a sign of the systemic toxicity of the treatments. The animals were weighed on the treatment starting date before plasmid injections and thereafter every second day until the end of the experiment when the tumor grew up to 450 mm^3 on average. To determine the antitumor effect of the treatment, a tumor growth delay evaluation was performed. Based on the tumor volume calculations (described in the paragraph above), a tumor doubling time (DT) was determined as the time in which the tumor doubled the volume from the initial day of the experiment. Growth delay (GD) was determined as the difference in the DT of each tumor in the therapeutic and mean DT in the control group [33]. The tumor growth delay assay was performed in the same animals used for CEUS measurements.

Mice with tumor regression were examined for tumor presence for 100 days after the treatment. If they were tumor free 100 days after the treatment, they were considered complete responders (CRs). They were challenged with a second subcutaneous injection of the melanoma cells as previously described. Animals without tumor growth in the subsequent 100 days were considered resistant to secondary challenges.

2.4. Histological analysis

From each experimental group, three tumors were collected for immunohistological (IHC) analysis on day 6 from the beginning of the therapy. The tumors were fixed in IHC zinc fixative (BD Biosciences, San Diego, CA, USA), embedded in paraffin blocks, and cut into 2-μm-thick sections, which were stained to determine blood vessels in the tumors. The sections were incubated with pri-

Table 1
Procedures performed in the twelve groups of mice with melanoma B16F10 treated with irradiation and gene electrotransfer (GET) of plasmid DNA encoding shRNA against MCAM.

	Treatment group	No. of included mice	Treatment	Treatment schedule
1	CTRL	9	no therapies performed	
2	pC	9	intratumoral injection of control plasmid DNA (pENTR/U6 pControl, 4 μg/μl) [17,19,22], 50 μg (12.5 μl)	on days 0, 2 and 4
3	pMCAM	9	intratumoral injection of plasmid DNA encoding shRNA MCAM (pENTR/U6 CD146, 4 μg/μl) [18], 50 μg (12.5 μl)	on days 0, 2 and 4
4	EP	9	8 square electric pulses of 600 V/cm, a pulse duration of 5 ms, and a frequency of 1 Hz	on days 0, 2 and 4
5	IR	9	irradiation in special lead holders with the apertures of 10 mm: a single dose of 15 Gy at a dose rate of 2.16 Gy/min	on day 1
6	GET pC	9	as described above for GET and pC: EP were delivered 10 min after intratumoral plasmid DNA injection	on days 0, 2 and 4
7	GET pMCAM	10	as described above for GET and pMCAM: EP were delivered 10 min after intratumoral plasmid DNA injection	on days 0, 2 and 4
8	EP IR	9	as described above for EP and IR	EP on days 0, 2, 4 IR on day 1
9	pMCAM IR	9	as described above for pMCAM and IR	pMCAM on days 0, 2, 4 IR on day 1
10	pC IR	9	as described above for pC and IR	pC on days 0, 2, 4 IR on day 1
11	GET pMCAM IR	10	as described above for GET pMCAM and IR	GET on days 0, 2, 4 IR on day 1
12	GET pC IR	9	as described above for GET pC and IR	GET pC on days 0, 2, 4 IR on day 1

LEGEND: CTRL = untreated control; GET = gene electrotransfer; EP = electric pulses; IR = single-dose irradiation; pC = intratumoral injection of control plasmid; pMCAM = intratumoral injection of plasmid DNA encoding shRNA for MCAM.

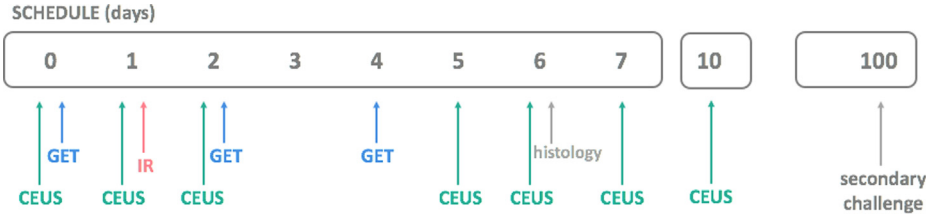

Scheme 1. Schedule of the experiment. CEUS = contrast-enhanced ultrasound, GET = gene electrotransfer of plasmid DNA, IR = irradiation (15 Gy).

mary rabbit polyclonal antibodies against CD31 (ab28364; Abcam, USA) at a dilution of 1:1000. Next, the sections were incubated with biotinylated goat anti-rabbit antibodies, streptavidin-peroxidase conjugate, and peroxidase substrate (rabbit-specific HRP/DAB detection IHC kit; ab64261; Abcam, USA), followed by hematoxylin counterstaining, as described previously [19]. Five randomly selected viable parts of each tumor were examined using a BX-51 microscope under 40 × magnification (numerical aperture 0.85) and captured using a DP72 CCD camera (both Olympus, Hamburg, Germany). The images were analyzed by two independent researchers and presented as the vascular density (the number of vessels per analyzed area, i.e., the number of vessels divided by the area of the acquired image).

2.5. Statistical analysis

The mean and standard deviation or error are considered measures of centrality and variability in numerical variables. One-way analysis of variance followed by the Holm–Sidak corrected t-tests were used to exploratory compare the mean differences in DT or vascular density between the treatment groups (Systat Software, Chicago, IL, USA). Generalized Bland–Altman plots were used to inspect the possible correlation between the mean values and their variability. Independent samples *t*-test was used to explore the possible daily difference between mean peak enhancement (PE) values in groups (CR vs. non-CR). The daily association between the PE and (log) DT values were explored using linear regression models and presented in scatterplots with linear regression lines. The p-values for each day were adjusted using Hommel's correction for the familywise error rate due to multiple comparisons. Additionally, to model a possible association of PE measurements over time with the status CR or non-CR, mixed-effect logistic regression was applied (considering each mouse and each treatment as random effects). Statistical package R was used [34]. Statistical significance was set to $p < 0.05$.

3. Results

To evaluate the capacity of CEUS to assess tumor perfusion/vascularization and outcome following electroporation treatment, we used mice bearing B16F10 melanoma tumors subjected to electroporation gene therapy and ionizing radiation as a that was previously observed to be a relevant model [18], where different levels of response were determined after monotherapies and after the combined treatment with radiation therapy. Ultrasound (US) system built-in software showed the perfusion curve and the following parameters: Base Intensity (BI: the basic intensity of non-contrast perfusion status), Peak Intensity (PI) and Area Under Curve (AUC). Peak Enhancement (PE) was calculated as the difference between PI and BI. PE and AUC are blood volume parameters. The parameters describing blood flow rate are Time To Peak (TTP:

the time at which contrast intensity reaches a peak), Ascending Slope (AS: the slope between the starting point of lesion perfusion and the peak), Arrival Time (AT: the time at which the contrast intensity appears, generally the current time value is 110% higher than the baseline intensity), Descend Time to one-half (DT/2: the time at which the intensity is half the value of the peak intensity), and Descending Slope (DS: the slope between the and the peak and ending point of lesion perfusion) (Fig. 1). No evident association was observed between vascular density (measured by IHC) and tumor growth (assessed by a caliper) and CEUS blood flow parameters (AT, AS, TTP, DT/2, DS) and AUC blood volume parameter; thus, only PE as the CEUS result was analyzed and is reported below.

3.1. Correlation of the CEUS results with the vascular density in tumors

To determine if CEUS could be used as a method to evaluate an antivascular response to treatment using GET of pMCAM and irradiation, the CEUS results were compared with the vascular density in histological tumor sections (Table 2). The mean vascular density for the combined therapeutic groups GET pMCAM IR, GET pMCAM and GET pC IR was significantly lower, from 1.4- to 3.8-fold than that in the pertinent control groups and untreated control group. The mean PE values for the combined therapeutic groups GET pMCAM IR, GET pMCAM and GET pC IR were significantly lower, from 1.8- to 6.9-fold, than those of the pertinent control groups (and untreated control group) (Table 2). The correlation of the histological results (vascular density) and PE was found for all the treatment groups (Supplementary Figure S2). Because the measurements of vascular density were mostly taken from different mice compared with the measurements of PE, none of the standard correlation measures between these two methods could be reported.

Comparing to pertinent and untreated control groups, in the combined therapeutic groups GET pMCAM IR, GET pMCAM and GET pC IR, a decrease in perfusion and a smaller number of blood vessels were observed by CEUS and histological analyses, respectively (Supplementary Figs. S1 and S2).

3.2. Heterogeneity of perfusion in tumors

Perfusion curves for different ROIs of the same tumor showed that the tumors that were larger than 40 mm^3 were commonly heterogeneously perfused (Supplementary Figure S3). Heterogeneous perfusion was more pronounced with the increased tumor volume in all the treatment groups. To inspect this heterogeneity, Bland–Altman plots of the means and standard deviations for each treatment group are presented in Fig. 2A for vascular density and Fig. 2B for PE. The variabilities increased in the treatment groups with a larger mean PE—i.e., the mice in groups with higher values of PE were more heterogeneous than mice in groups with lower PE values.

Heterogenous perfusion of the tumors in the same therapeutic group on the same day is also observed in Supplementary Figure S4. Heterogeneity of perfusion was also commonly observed for the same tumor during the time of observation and an example of such a tumor, where complete response was observed, can be seen in Supplementary Figure S5.

Table 2
Mean values and standard errors for CEUS peak enhancement (PE) and vessel density in the twelve treatment groups on day 6 after the treatment.

Treatment group	CEUS PE		Vessel density (number/mm^2)	
	Mean	SE	Mean	SE
CTRL	10.4	0.7	364.3	21.1
pC	9.6	1.9	331.1	33.2
pMCAM	9.3	0.8	326.8	20.6
EP	8.4	2.2	280.9	18.4
IR	6.5	0.5	211.5*	12.1
GET pC	6.7	2.2	248.5*	29.8
GET pMCAM	2.4*	0.8	127.1*	11.7
pC IR	4.2*	0.2	172.1*	12.9
pMCAM IR	5.1	2.2	175.8*	13.9
EP IR	5.7	1.1	203.0*	16.3
GET pC IR	2.3*	1.1	127.4*	13.2
GET pMCAM IR	1.5*	0.5	96.0*	7.7

LEGEND: CTRL = untreated control; GET = gene electrotransfer; IR = single-dose irradiation, 15 Gy; pC = intratumoral injection of control plasmid; pMCAM = intratumoral injection of plasmid DNA encoding shRNA for MCAM; PE = peak enhancement; SE = standard error of arithmetic mean.
* $p < 0.05$ = statistically significant mean difference compared with untreated control group.

3.3. Tumor growth delay after the silencing of MCAM and irradiation

The growth of B16F10 melanoma after silencing MCAM and irradiation is shown in Table 3 and Supplementary Figure S6. Monotherapies, EP or IR or the injection of either plasmid showed no significant effect on tumor growth compared with control untreated tumors. Furthermore, partially combined treatments of

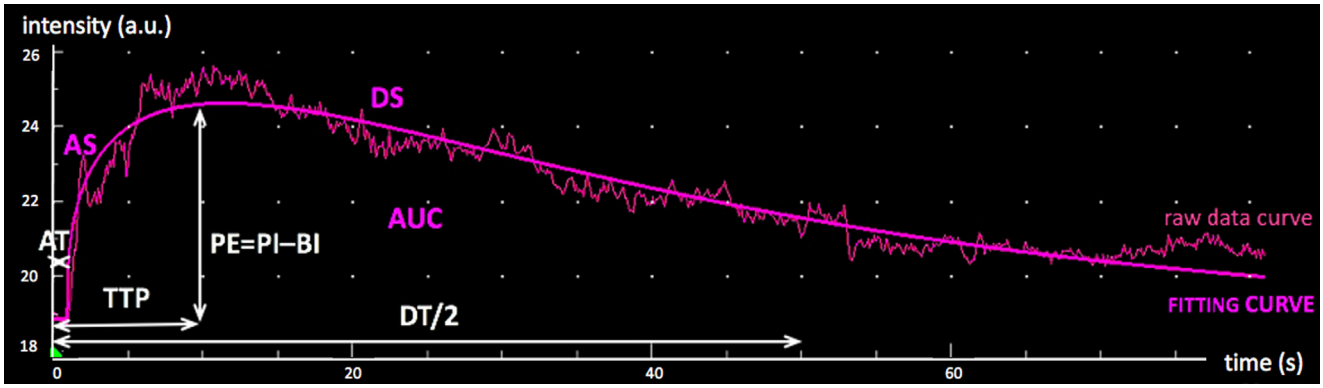

Fig. 1. CEUS perfusion curve with a schematic representation of the dynamic parameters. Raw data and fitting curves are displayed by the built-in software of the M9 ultrasound device (Mindray). Peak enhancement (PE) is the difference between peak (PI) and Base Intensity (BI). Arrival Time (AT) is the time after contrast injection until the contrast agent appears. Time to peak (TTP) is the time at which the contrast intensity reaches a peak value. Descend Time to one-half (DT/2) is the time when the intensity is one-half the value of the peak intensity. Ascending and dDescending Slope (AS and DS) refer to slope coefficients. Area Under the Curve (AUC) is the area under the perfusion curve.

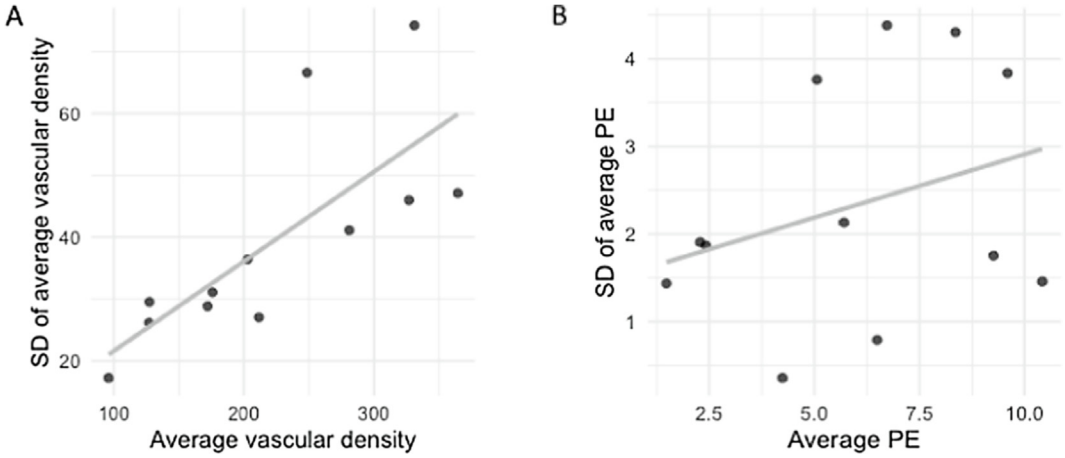

Fig. 2. Bland-Altman Plots of the means and standard deviations of vascular density (A) and CEUS peak enhancement (PE) at day 6 for all treatment groups. The gray lines are for visual inspection only.

Table 3
Antitumor response of B16F10 melanoma after different treatment modalities.

Group	n	DT (days)		GD (days)		CR		resistant to SC	
		Mean	SE	Mean	SE	n	%	n	%
CTRL	6	1.3[#]	0.2	/	/	0	0	0	0
pC	6	2.6[#]	0.3	1.3[#]	0.3	0	0	0	0
pMCAM	6	2.5[#]	0.5	1.2[#]	0.5	0	0	0	0
EP	6	3.6[#]	1.6	2.3[#]	1.6	0	0	0	0
IR	6	1.4[#]	0.3	0.1[#]	0.3	0	0	0	0
GET pC	6	34.3[*,#]	0.8	33.0[*,#]	0.8	1	20.0	0	0
GET pMCAM	7	37.1[*]	20.7	35.8[*]	20.7	1	14.3	1	100
pC IR	6	5.8[*,#]	1.7	4.5[*,#]	1.7	0	0	0	0
pMCAM IR	6	23.0[*,#]	14.7	21.6[*,#]	14.7	1	16.7	1	100
EP IR	6	8.5[*,#]	2.3	7.2[*,#]	2.3	0	0	0	0
GET pC IR	5	74.2[*]	23.8	72.9[*]	23.8	2	40.0	2	100
GET pMCAM IR	7	80.4[*]	19.6	79.1[*]	19.6	3	42.9	3	100

LEGEND: CR = complete response, tumor-free animal at day 100; CTRL = untreated control; DT = tumor doubling time; EP = application of electrical pulses; GD = tumor growth delay (=$DT_{tumor\ in\ experimental\ group}$–mean of DT_{ctrl}); GET = gene electrotransfer; IR = single-dose irradiation, 15 Gy; n = number of all mice in group; pC = intratumoral injection of control plasmid; pMCAM = intratumoral injection of plasmid DNA encoding shRNA for MCAM; SC = mice resistant to secondary challenge; SE = standard error of arithmetic mean; / = not applicable.

[*] $p < 0.05$ = statistically significant mean difference compared to control.

[#] $p < 0.05$ = statistically significant mean difference compared to GET pMCAM IR, GET pC IR.

tumors (EP IR, GET pMCAM, GET pC, pMCAM IR, pC IR, GET pMCAM, GET pC) significantly prolonged tumor growth delay compared with the control tumors. Additionally, tumor cures were obtained in the controls of GET pMCAM, GET pC and pMCAM IR, ranging from 14% to 20% (Table 3). When a single dose of IR was combined with GET pMCAM or GET pC, pronounced radiosensitization was observed compared with the control, monotherapy, EP IR, pMCAM IR, and pC IR groups, resulting in a significant reduction of tumor growth (43%) and a tumor cure rate of 40%; additionally, the tumors were resistant to secondary challenge (Table 3).

Irradiation alone or combined treatments resulted in hair loss, but no skin desquamation was observed. Additionally, no systemic toxicity was observed after the treatments.

3.4. CEUS PE capacity to predict antitumor response to treatment

To explore the capacity of CEUS to predict tumor outcome, we compared CEUS PE values and growth parameters (CR, DT, GD, resistance to secondary challenge). Among the mice with CEUS results (n = 49), 8 were complete responders: three in the GET pMCAM IR group, one in the GET pMCAM group, one in the GET pC group, two in the GET pC IR group, and one in the pMCAM IR group (Table 3).

The comparisons of mean PE values between the CR and non-CR groups demonstrated that the mean PE values were significantly lower in the CR group from day 5 (Supplementary Table S1). The association between the daily CEUS PE parameter and logarithmically transformed DT is explored graphically in Fig. 3. Note that the mice with the most advanced tumors (with the shortest DT values) were excluded from the analyses early (as shown on days 6 and 7 by the lack of dots with small DT values); the CR mice had DT ceiled to 100. The results of linear regression analyses for each day of measurement associating PE with logarithmically transformed DT are presented in Supplementary Table S2. Negative regression coefficients suggest that the larger is the PE of a mouse the lower is the expected (log) DT. Similar findings were observed as above, when evaluating the association with CR.

An additional attempt to model a possible association of PE measurements over time with the status CR or non-CR by mixed-effects logistic regression showed no statistically significant predictors. This finding can be partially attributed to the lack of strength in detecting a difference in the early days and bias introduced in the sample in the later days. However, the trends for our data set stayed the same as in the simpler analyses above—i.e., the larger is the PE, the less probable is the CR at a fixed day.

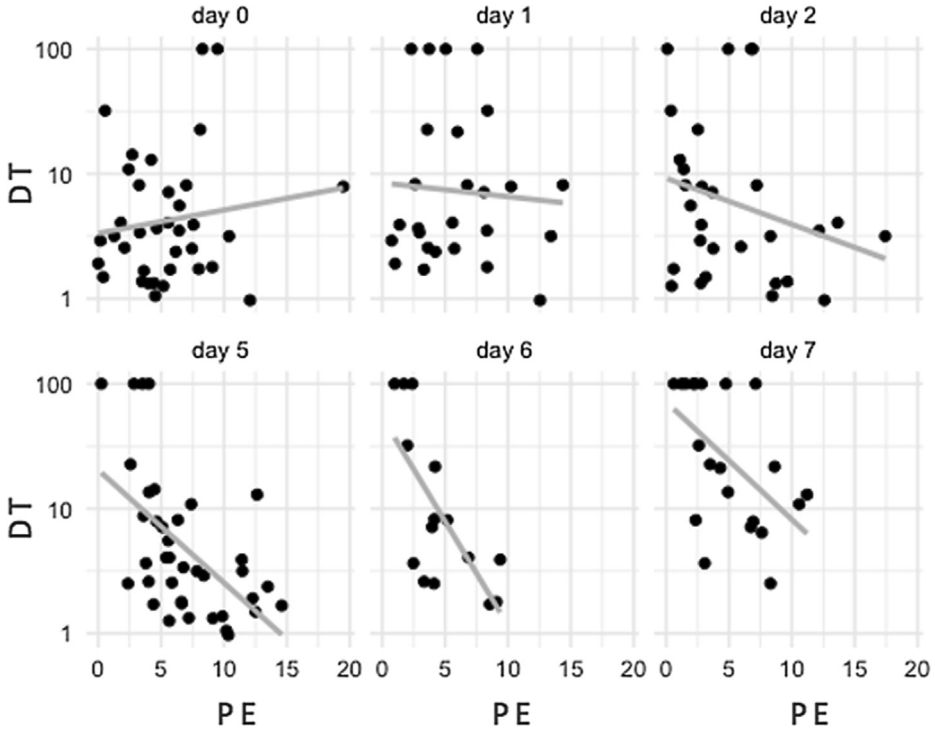

Fig. 3. Association between CEUS peak enhancement (PE) and logarithmically transformed doubling time (DT). The lines serve as visual inspection.

4. Discussion

In the current study, among the CEUS parameters only PE was an indicator of treatment response in the murine model and correlated with mean vascular density in histological analyses of treated tumors. The mean PE values were significantly lower in the tumors that responded to therapy with CR. In addition, PE values showed a trend toward correlation with antitumor efficacy (the greater the PE value of a mouse, the lower the expected DT value and a lower probability of CR). Thus, this study confirms that CEUS could be used to evaluate perfusion and treatment response in mice treated with vascular targeted therapies that have anti-angiogenic and anti-vascular activities [1,35].

Tumor perfusion can be assessed by various methods investigating tumor vasculature and tumor perfusion, either invasively (e.g., histological analyses) or less invasively (e.g., contrast-enhanced imaging). CEUS is a simple method of perfusion assessment, and our data show that CEUS evaluation agrees with the histological analyses of tumor blood vessels abundance, a finding that is consistent with other studies, both preclinical [2–4] and clinical [6–9]. The significantly lower PE values for CR tumors and the tendency for CEUS results to correlate with treatment outcome in our study are consistent with preclinical murine [3,4] and human clinical studies [10–13] in which CEUS results are a useful predictor of antiangiogenic treatment. However, in studies of canine tumors treated with radiotherapy, CEUS was not found to be predictive [36,37]. The canine studies included a small number of dogs with different tumor types treated with radiotherapy, and the reason why CEUS was not predictive may also be due to the different mechanism of antitumor action between radiotherapy alone and in combination with EP–based treatment. Radiation therapy is more efficient in areas with increased perfusion because hypoxic cells are resistant to treatment. Furthermore, only combined therapy is an antiangiogenic treatment [18–20].

In human clinical studies [10–13], different CEUS parameters (AUC, TTP, AS, and PE) showed trends toward a correlation with survival. In our study, the CEUS parameter that correlated with histology and tumor growth was PE, a parameter that describes the blood volume of the investigated area. On the other hand, parameters that describe the blood flow rate did not show associations with tumor growth and histological results. Possible reasons for this lack of correlation could be the retroorbital injections of contrast without the use of an infusion pump and different planes of anesthesia. The latter influences physiologic parameters such as the systemic blood pressure, body temperature, heart rate, cardiac contractility, and others, which all affect tissue perfusion, which depends on cardiac, vascular, microcirculatory, and humoral factors. Retroorbital injections of contrast agents were shown to be comparable with tail injections in mice [38]; however, in that study, contrast agents were administered via a catheter; in our study, the operator inserted the needle into the retro-orbital sinus [32]. Furthermore, the rate of contrast injection was less unified than that using an infusion pump.

The tumor vasculature differs from the normal vasculature; the former is immature with a poorly developed discontinuous endothelial-cell lining, and the basement membrane is irregular and structurally abnormal. Tumor vascular networks are chaotic, and the flow through many of the tumor vessels is only intermittent [1,35,39]. These characteristics of tumor vessels contribute to spatial and temporal heterogeneity in the tumor blood flow [39], as observed in our study; the tumors were commonly heterogeneously perfused, and the perfusion of the same tumor was different on different days. Regions of the tumor that are poorly perfused are radioresistant; therefore, combined treatments with vascular targeted therapies aiming to normalize the tumor vasculature are intensively investigated. In our study, the CEUS results and histological vascular density showed that GET of plasmid DNA encoding shRNA for MCAM and GET of control plasmid both exhibit radiosensitizing effects. Electric pulses of a voltage higher than 560 V induce a local blood flow modifying effect or 'vascular lock', which is characterized by vasoconstriction and increased wall permeabilization of small blood vessels, resulting in tissue

edema [40–50]. The duration and strength of vascular lock depend on EP (number, amplitude, and duration), type of tissue (healthy versus tumor cells), and use of chemotherapeutics [43–46]. Blood flow is slowly restored after EP; in 24 h, it approaches the flow before EP [45–49]. CEUS has been used to describe decreased perfusion after electrochemotherapy (ECT) of human hepatic tumors [51] and after the ECT of healthy porcine liver [52]. However, these immediate effects after EP were not evident in this study because CEUS was performed on each day before the therapies to evaluate the vascular effects of 24-hour combined treatment.

The reasons for the first major limitation of this study—the small number of animals and measurements—were the principle of 3Rs (Reduce, Reuse and Recycle) and exclusion of measurements due to the unpredictable contrast stability. The chemical and physical stabilities of the Sonovue microbubble dispersion last for 6 h, and ultrasound contrast agents are easily destroyed in small-gauge needles [53]. Both reasons for the first major limitation are also reasons for the second major limitation of this study, which was that not all of the measurements of vascular density measurements were obtained from the same mice that were subjected to the PE measurements; therefore, none of the standard correlation measures could be reported. However, the mice were inbred syngenic animals, indicating more genetic uniformity and pathophysiological similarity among individuals [54]. In the treatment groups using therapeutic plasmid—i.e., GET pMCAM and GET pMCAM IR—vascular density and PE were determined in the same mice. The scatterplot of these measurements and Pearson's correlation are reported in the Supplementary Information (Supplementary Figure S7).

5. Conclusion

CEUS results for tumors correlated with histological analysis of blood vessel density, demonstrating they could be a valuable method of tissue perfusion assessment. Furthermore, CEUS results for tumors that responded to therapy with CR were significantly different from those without CR and CEUS results showed a trend toward correlation with antitumor effectiveness. In a patient evaluation, simple methods such as CEUS, which provide readily available data during therapy and can be repeated frequently are advantageous because they could provide beneficial prognostic and predictive information, assisting the clinician in deciding whether the repetition of therapy is necessary for the response to therapy. Had the number of mice in this study been larger, the observed tendency of CEUS results to correlate with antitumor efficacy could have been more categorical. The potential value of CEUS as a technique to determine prognosis and predict outcome of neoplastic disease warrants further studies in scientific research and clinical practice to confirm whether it can predict the disease outcome and assist in the planning of repeated therapy or different treatment combinations in individual patients.

Declaration of Competing Interest

The authors declare that they have no known competing financial interests or personal relationships that could have appeared to influence the work reported in this paper.

Acknowledgments

The authors thank Miha Melinec and Tone Jamnik (DIPROS d.o.o.) for their assistance and ultrasonographic machines that enabled contrast studies. Language editing services for this manuscript were provided by American Journal Experts.

Funding

Furthermore, we acknowledge the financial support of the Slovenian Research Agency (research program No. P3-003 and No. P4-0053). The funder had no role in the study design, data collection and analysis, decision to publish, or preparation of the manuscript.

Authors' contributions

Study concepts/study design, S.K.B., D.P., M.C., G.S.; data acquisition, M.B., S.K.B, M.Bo.; data analysis/interpretation, M.B., N.B., D. P., N.K., S.K.B,; manuscript drafting, M.B., N.B., D.P., S.K.B; manuscript revision for important intellectual content, M.C., G.S., S.K.B, D.P.; approval of the final submitted manuscript, all authors; and manuscript editing, all authors.

References

[1] G.M. Tozer, C. Kanthou, B.C. Baguley, Disrupting tumour blood vessels, Nat. Rev. Cancer 5 (6) (2005) 423–435, https://doi.org/10.1038/nrc1628.
[2] E.F. Donnelly, L. Geng, W.E. Wojcicki, A.C. Fleischer, D.E. Hallahan, Quantified power Doppler US of tumor blood flow correlates with microscopic quantification of tumor blood vessels, Radiol 219 (1) (2001) 166–170, https://doi.org/10.1148/radiology.219.1.r01ap38166.
[3] J.H. Zhou, L.H. Cao, J.B. Liu, W. Zheng, M. Liu, R.Z. Luo, F. Han, A. Li, Quantitative assessment of tumor blood flow in mice after treatment with different doses of an antiangiogenic agent with contrast-enhanced destruction-replenishment US, Radiology 259 (2) (2011) 406–413, https://doi.org/10.1148/radiol.10101339.
[4] J.H. Zhou, L.H. Cao, W. Zheng, M. Liu, F. Han, A.H. Li, Contrast-enhanced gray-scale ultrasound for quantitative evaluation of tumor response to chemotherapy: preliminary results with a mouse hepatoma model, AJR Am. J. Roentgenol. 196 (1) (2011) W13–7, https://doi.org/10.2214/AJR.10.4734.
[5] K.J. Nierman, A.C. Fleischer, J. Huamani, T.E. Yankeelov, D.W. Kim, W.D. Wilson, D.E. Hallahan, Measuring tumor perfusion in control and treated murine tumors: correlation of microbubble contrast-enhanced sonography to dynamic contrast-enhanced magnetic resonance imaging and fluorodeoxyglucose positron emission tomography, J. Ultrasound Med. 26 (6) (2007) 749–756, https://doi.org/10.7863/jum.2007.26.6.749.
[6] J.P. Sedelaar, G.J. van Leenders, C.A. Hulsbergen-van de Kaa, H.G. van der Poel, J. A. van der Laak, F.M. Debruyne, H. Wijkstra, J.J. de la Rosette, Microvessel density: correlation between contrast ultrasonography and histology of prostate cancer, Eur. Urol. 40 (3) (2001) 285–293, https://doi.org/10.1159/000049788.
[7] X. Leng, G. Huang, F. Ma, L. Yao, Regional Contrast-Enhanced Ultrasonography (CEUS) characteristics of breast cancer and correlation with Microvessel Density (MVD), Med. Sci. Monit. 23 (2017) 3428–3436, https://doi.org/10.12659/MSM.901734.
[8] X. Li, Y. Li, Y. Zhu, L. Fu, P. Liu, Association between enhancement patterns and parameters of contrast-enhanced ultrasound and microvessel distribution in breast cancer, Oncol Lett 15 (4) (2018) 5643–5649, https://doi.org/10.3892/ol.2018.8078.
[9] S. Ohlerth, M. Wergin, C.R. Bley, F. Del Chicca, D. Laluhova, B. Hauser, M. Roos, B. Kaser-Hotz, Correlation of quantified contrast-enhanced power Doppler ultrasonography with immunofluorescent analysis of microvessel density in spontaneous canine tumours, Vet. J. 183 (1) (2010) 58–62, https://doi.org/10.1016/j.tvjl.2008.08.026.
[10] N. Lassau, S. Koscielny, L. Albiges, L. Chami, B. Benatsou, M. Chebil, A. Roche, B. J. Escudier, Metastatic Renal Cell Carcinoma Treated with Sunitinib: Early Evaluation of Treatment Response Using Dynamic Contrast-Enhanced Ultrasonography, Clin Canc Res 16 (4) (2010) 1216–1225, https://doi.org/10.1158/1078-0432.CCR-09-2175.
[11] N. Lassau, S. Koscielny, L. Chami, M. Chebil, B. Benatsou, A. Roche, M. Ducreux, D. Malka, V. Boige, Advanced hepatocellular carcinoma: early evaluation of response to bevacizumab therapy at dynamic contrast-enhanced US with quantification – preliminary results, Radiology 258 (1) (2011) 291–300, https://doi.org/10.1148/radiol.10091870.
[12] N. Lassau, J. Bonastre, M. Kind, V. Vilgrain, J. Lacroix, M. Cuinet, S. Taieb, R. Aziza, A. Sarran, C. Labbe-Devilliers, B. Gallix, O. Lucidarme, Y. Ptak, L. Rocher, L.M. Caquot, S. Chagnon, D. Marion, A. Luciani, S. Feutray, J. Uzan-Augui, B. Coiffier, B. Benastou, S. Koscielny, Validation of dynamic contrast-enhanced ultrasound in predicting outcomes of antiangiogenic therapy for solid tumors: the French multicenter support for innovative and expensive techniques study, Invest. Radiol. 49 (12) (2014) 794–800, https://doi.org/10.1097/RLI.0000000000000085.
[13] N. Lassau, B. Coiffier, M. Kind, V. Vilgrain, J. Lacroix, M. Cuinet, S. Taieb, R. Aziza, A. Sarran, C. Labbe-Devilliers, B. Gallix, O. Lucidarme, Y. Ptak, L. Rocher, L.M. Caquot, S. Chagnon, D. Marion, A. Luciani, S. Feutray, J. Uzan-Augui, B. Benatsou, J. Bonastre, S. Koscielny, Selection of an early biomarker for vascular

normalization using dynamic contrast-enhanced ultrasonography to predict outcomes of metastatic patients treated with bevacizumab, Ann. Oncol. 27 (10) (2016) 1922–1928, https://doi.org/10.1093/annonc/mdw280.
[14] M. Cemazar, T. Jarm, G. Sersa, Cancer electrogene therapy with interleukin-12, Curr Gene Ther 10 (4) (2010) 300–311, https://doi.org/10.2174/156652310791823425.
[15] M. Cemazar, J. Ambrozic Avgustin, D. Pavlin, G. Sersa, A. Poli, A. Krhac Levacic, N. Tesic, U. Lampreht Tratar, M. Rak, N. Tozon, Efficacy and safety of electrochemotherapy combined with peritumoral IL-12 gene electrotransfer of canine mast cell tumours, Vet. Comp. Oncol. 15 (2) (2017) 641–654, https://doi.org/10.1111/vco.2017.15.issue-210.1111/vco.12208.
[16] A.I. Daud, R. DeConti, S. Andrews, P. Urbas, A.I. Riker, V.K. Sondak, P.N. Munster, D.M. Sullivan, K.E. Ugen, J.L. Messina, R. Heller, Phase I trial of interleukin-12 plasmid electroporation in patients with metastatic melanoma, J Clin Oncol 26 (36) (2008) 5896–5903, https://doi.org/10.1200/JCO.2007.15.6794.
[17] L. Prosen, B. Markelc, T. Dolinsek, B. Music, M. Cemazar, G. Sersa, Mcam silencing with RNA interference using magnetofection has antitumor effect in murine melanoma, Mol. Ther. Nucleic Acids 3 (2014) e205, https://doi.org/10.1038/mtna.2014.56.
[18] S. Kranjc Brezar, V. Mrak, M. Bosnjak, M. Savarin, G. Sersa, M. Cemazar, Intratumoral gene electrotransfer of plasmid DNA encoding shRNA against melanoma cell adhesion molecule radiosensitizes tumors by antivascular effects and activation effects and activation of an immune response, Vaccines 135 (2020), https://doi.org/10.3390/vaccines8010135.
[19] M. Savarin, U. Kamensek, M. Cemazar, R. Heller, G. Sersa, Electrotransfer of plasmid DNA radiosensitizes B16F10 tumors through activation of immune response, Radiol. Oncol. 51 (2017) 30–39, https://doi.org/10.1515/raon-2017-0011.
[20] G. Tevz, S. Kranjc, M. Cemazar, U. Kamensek, A. Coer, M. Krzan, S. Vidic, D. Pavlin, G. Sersa, Controlled systemic release of interleukin-12 after gene electrotransfer to muscle for cancer gene therapy alone or in combination with ionizing radiation in murine sarcomas, J. Gene. Med. 11 (12) (2009) 1125–1137, https://doi.org/10.1002/jgm.v11:1210.1002/jgm.1403.
[21] A. Sedlar, S. Kranjc, T. Dolinšek, M. Čemažar, A. Coer, G. Serša, Radiosensitizing effect of intratumoral interleukin-12 gene electrotransfer in murine sarcoma, BMC Cancer 13 (2013) 38, https://doi.org/10.1186/1471-2407-13-38.
[22] M. Stimac, U. Kamensek, M. Cemazar, S. Kranjc, A. Coer, G. Sersa, Tumor radiosensitization by gene therapy against endoglin, Cancer Gene Ther 23 (7) (2016) 214–220, https://doi.org/10.1038/cgt.2016.20.
[23] M. Savarin, A. Prevc, M. Rzek, M. Bosnjak, I. Vojvodic, M. Cemazar, T. Jarm, G. Sersa, Intravital monitoring of vasculature after targeted gene therapy alone or combined with tumor irradiation, Technol Cancer Res Treat 17 (2) (2018), https://doi.org/10.1177/1533033818784208.
[24] M. Bosnjak, T. Jesenko, U. Kamensek, G. Sersa, J. Lavrencak, L. Heller, M. Cemazar, Electrotransfer of different control plasmids elicits antitumor effectiveness in B16.F10 melanoma, Cancers 10 (2) (2018) 37, https://doi.org/10.3390/cancers10020037.
[25] L.C. Heller, R. Heller, Electroporation gene therapy preclinical and clinical trials for melanoma, Curr Gene Ther 10 (4) (2010) 312–317, https://doi.org/10.2174/156652310791823489.
[26] L. Heller, V. Todorovic, M. Cemazar, Electrotransfer of single-stranded or double-stranded DNA induces complete regression of palpable B16.F10 mouse melanomas, Cancer Gene Ther. 20 (12) (2013) 695–700, https://doi.org/10.1038/cgt.2013.71.
[27] S. Kranjc, M. Cemazar, A. Grosel, M. Sentjurc, G. Sersa, Radiosensitising effect of electrochemotherapy with bleomycin in LPB sarcoma cells and tumors in mice, BMC Cancer 5 (2005) 115–123, https://doi.org/10.1186/1471-2407-5-115.
[28] S. Kranjc, G. Tevz, U. Kamensek, S. Vidic, M. Cemazar, G. Sersa, Radiosensitizing effect of electrochemotherapy in a fractionated radiation regimen in radiosensitive murine sarcoma and radioresistant adenocarcinoma tumor model, Radiat. Res. 172 (6) (2009) 677–685.
[29] C. Dietrich, M. Averkiou, J.-M. Correas, N. Lassau, E. Leen, F. Piscaglia, An EFSUMB introduction into Dynamic Contrast- Enhanced Ultrasound (DCE-US) for quantification of tumour perfusion, Ultraschall Med. 33 (04) (2012) 344–351, https://doi.org/10.1055/s-0032-1313026.
[30] F. Piscaglia, C. Nolsoe, C.F. Dietrich, D.O. Cosgrove, O.H. Gilja, M. Bachmann Nielsen, T. Albrecht, L. Barozzi, M. Bertolotto, O. Catalano, M. Claudon, D.A. Clevert, J.M. Correas, M. D'Onofrio, F.M. Drudu, Y. Eyding, M. Giovannini, M. Hocke, A. Ignee, E.M. Jung, A.S. Klauser, N. Lasssau, E. Leen, G. Mathis, A. Saftoiu, G. Seidel, P.S. Sidhu, G. ter Haar, D. Timmerman, H.P. Weskott, The EFSUMB Guidelines and Recommendations on the Clinical Practice of Contrast Enhanced Ultrasound (CEUS): update 2011 on non-hepatic applications, Ultraschall Med. 33 (1) (2012) 33–59, https://doi.org/10.1055/s-0031-1281676.
[31] M. Westwood, M. Joore, J. Grutters, K. Redekop, N. Armstrong, K. Lee, V. Gloy, H. Raatz, K. Misso, J. Severens, J. Kleijnen, Contrast-enhanced ultrasound using SonoVue® (sulphur hexafluoride microbubbles) compared with contrast-enhanced computed tomography and contrast-enhanced magnetic resonance imaging for the characterisation of focal liver lesions and detection of liver metastases: a systematic review and cost-effectiveness analysis, Health Technol. Assess. 17 (16) (2013) 1–243, https://doi.org/10.3310/hta17160.
[32] T. Yardeni, M. Eckhaus, H.D. Morris, M. Huizing, S. Hoogstraten-Miller, Retro-orbital injections in mice, Lab Anim (NY) 40 (5) (2011) 155–160, https://doi.org/10.1038/laban0511-155.
[33] Demidenko E. Three endpoints of in vivo tumour radiobiology and their statistical estimation. Int J Radiat Biol 2010; 86(2): 164–73. doi: 10.3109/09553000903419304.
[34] R Core Team (2020). R: A language and environment for statistical computing. R Foundation for Statistical Computing, Vienna, Austria. https://www.R-project.org [15th June 2020].
[35] R.K. Jain, Normalization of tumor vasculature: an emerging concept in antiangiogenic therapy, Science 307 (5706) (2005) 58–62, https://doi.org/10.1126/science.1104819.
[36] C. Rohrer Bley, D. Laluhova, M. Roos, B. Kaser-Hotz, S. Ohlerth, Correlation of pretreatment polarographically measured oxygen pressures with quantified contrast-enhanced power doppler ultrasonography in spontaneous canine tumors and their impact on outcome after radiation therapyKorrelation des polarographisch gemessenen Sauerstoffdrucks mit quantifiziertem, kontrastverstärktem Power-Doppler-Ultraschall bei spontanen kaninen Tumoren und deren Einfluss auf das Tumorverhalten nach Strahlentherapie, Strahlenther. Onkol. 185 (11) (2009) 756–762, https://doi.org/10.1007/s00066-009-1988-6.
[37] S. Ohlerth, C.R. Bley, D. Laluhová, M. Roos, B. Kaser-Hotz, Assessment of changes in vascularity and blood volume in canine sarcomas and squamous cell carcinomas during fractionated radiation therapy using quantified contrast-enhanced power Doppler ultrasonography: a preliminary study, Vet. J. 186 (1) (2010) 58–63, https://doi.org/10.1016/j.tvjl.2009.07.006.
[38] F. Wang, M. Nojima, Y. Inoue, K. Ohtomo, S. Kiryu, Assessment of MRI contrast agent kinetics via retro-orbital injection in mice: comparison with tail vein injection, PLoS One 10 (6) (2015), https://doi.org/10.1371/journal.pone.0129326 e0129326.
[39] D.W. Siemann, The unique characteristics of tumor vasculature and preclinical evidence for its selective disruption by tumor-vascular disrupting agents, Cancer Treat. Rev. 37 (1) (2011) 63–74, https://doi.org/10.1016/j.ctrv.2010.05.001.
[40] G. Sersa, M. Cemazar, D. Miklavcic, DJ. Chaplin, Tumor blood flow modifying effect of electrochemotherapy with bleomycin, Anticancer Res 19 (1999) 4017–4022, https://doi.org/10.1007/978-3-540-73044-6 152.
[41] G. Sersa, M. Cemazar, C.S. Parkins, D.J. Chaplin, Tumour blood flow changes induced by application of electric pulses, Eur J Cancer 35 (1999) 672–677, https://doi.org/10.1016/S0959-8049(98)00426-2.
[42] J. Gehl, T. Skovsgaard, L.M. Mir, Vascular reactions to in vivo electroporation: characterization and consequences for drug and gene delivery, BBA 1569 (1–3) (2002) 51–58, https://doi.org/10.1016/s0304-4165(01)00233-1.
[43] G. Sersa, M. Cemazar, D. Miklavcic, Tumor blood flow modifying effects of electrochemotherapy: a potential vascular targeted mechanism, Radiol Oncol 37 (2003) 43–48, https://doi.org/10.1007/978-3-540-73044-6_153.
[44] G. Sersa, T. Jarm, T. Kotnik, A. Coer, M. Podkrajsek, M. Sentjurc, D. Miklavcic, M. Kadivec, S. Kranjc, A. Secerov, M. Cemazar, Vascular disrupting action of electroporation and electrochemotherapy with bleomycin in murine sarcoma, Br. J. Cancer 98 (2) (2008) 388–398, https://doi.org/10.1038/sj.bjc.6604168.
[45] T. Jarm, M. Cemazar, D. Miklavcic, G. Sersa, Antivascular effects of electrochemotherapy: implications in treatment of bleeding metastases, Expert Rev. Anticancer Ther. 10 (5) (2010) 729–746, https://doi.org/10.1586/era.10.43.
[46] E. Raesi, S.M.P. Firoozabadi, S. Hajizadeh, H. Rajabi, Z.M. Hassan, The effect of high-frequency electric pulses on tumor blood flow in vivo, J. Membrane Biol. 236 (1) (2010) 163–166, https://doi.org/10.1007/s00232-010-9288-8.
[47] E. Bellard, B. Markelc, S. Pelofy, F. Le Guerroué, G. Sersa, J. Teissié, M. Cemazar, M. Golzio, Intravital microscopy at the single vessel level brings new insights of vascular modification mechanisms induced by electropermeabilization, J. Control. Release 163 (3) (2012) 396–403, https://doi.org/10.1016/j.jconrel.2012.09.010.
[48] B. Markelc, E. Bellard, G. Serša, S. Pelofy, J. Teissie, A. Coer, M. Golzio, M. Cemazar, In vivo molecular imaging and histological analysis of changes induced by electric pulses used for plasmid DNA electrotransfer to the skin: a study in a dorsal window chamber in mice, J. Membr. Biol. 245 (9) (2012) 545–554, https://doi.org/10.1007/s00232-012-9435-5.
[49] B. Markelc, G. Sersa, M. Cemazar, Differential mechanisms associated with vascular disrupting action of electrochemotherapy: intravital microscopy on the level of single normal and tumor blood vessels, PLoS One 8 (2013), https://doi.org/10.1371/journal.pone.0059557 e59557.
[50] B. Markelc, E. Bellard, G. Sersa, T. Jesenko, S. Pelofy, J. Teissie, R. Frangez, M.P. Rols, M. Cemazar, M. Golzio, Increased permeability of blood vessels after reversible electroporation is facilitated by alterations in endothelial cell-to-cell junctions, J. Control. Release 276 (2018) 30–41, https://doi.org/10.1016/j.jconrel.2018.02.032.
[51] N. Boc, I. Edhemovic, B. Kos, M.M. Music, E. Brecelj, B. Trotovsek, M. Bosnjak, M. Djokic, D. Miklavcic, M. Cemazar, G. Sersa, Ultrasonographic changes in the liver tumors as indicators of adequate tumor coverage with electric field for effective electrochemotherapy, Radiol Oncol 52 (2018) 383–391, https://doi.org/10.2478/raon-2018-0041.
[52] M. Brloznik, N. Boc, G. Sersa, J. Zmuc, G. Gasljevic, A. Seliskar, R. Dezman, I. Edhemovic, N. Milevoj, T. Plavec, V. Erjavec, D. Pavlin, M. Bosnjak, E. Brecelj, U. Lampreht Tratar, B. Kos, J. Izlakar, M. Stukelj, D. Miklavcic, M. Cemazar, Radiological findings of porcine liver after electrochemotherapy with bleomycin, Radiol. Oncol. 53 (4) (2019) 415–426.
[53] D.B. Erlichman, A. Weiss, M. Koenigsberg, M.W. Stein, Contrast enhanced ultrasound: A review of radiology applications, Clin. Imaging 60 (2) (2019) 209–215, https://doi.org/10.1016/j.clinimag.2019.12.013.

[54] E. Costa, T. Ferreira-Gonçalves, G. Chasqueira, A.S. Cabrita, I.V. Figueiredo, R.C. Pinto, Experimental models as refined translational tools for breast cancer research, Sci. Pharm. 88 (2020) 32, https://doi.org/10.3390/scipharm88030032.

Maja Brloznik graduated as a Doctor of Veterinary Medicine and received her M.Sc. from the University of Ljubljana. She graduated at the University of Luxembourg as European Master of Small Animal Veterinary Medicine in 2018. She works in cardiology and diagnostic ultrasound at Small Animal Clinic of Veterinary Faculty of the University in Ljubljana and at International Veterinary Services in Asia. She is currently enrolled in PhD studies and her main research interests are radiologic methods as predictive factors of electrochemotherapy and gene therapy of murine and spontaneous canine tumors.

Nina Boc graduated as a Medical Doctor from the Medical faculty of University of Ljubljana. She earned her specialist degree in Radiology with honour in 2010. She is currently the head of the Radiology Department of Institute of Oncology in Ljubljana. Her main research interest is use of radiologic methods in electrochemotherapy. She is involved in various multicentre clinical studies.

Maja Cemazar received her Ph.D. in Basic Medical Sciences from the Medical Faculty, the University of Ljubljana in 1998. She works at the Department of Experimental Oncology, Institute of Oncology Ljubljana, and teaches at the Faculty of Health Sciences, University of Primorska, Slovenia. Her main research interests are in the field of gene electrotransfer employing plasmid DNA encoding different immunomodulatory and antiangiogenic therapeutic genes. In 2006 she received the Award of the Republic of Slovenia for important achievements in scientific research and development in the field of experimental oncology.

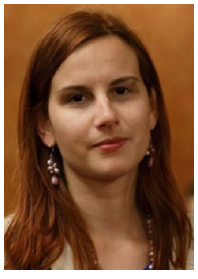

Masa Bosnjak received her Ph.D. in Basic Medical Sciences from the Medical Faculty, the University of Ljubljana in 2015. She is employed at the Institute of Oncology Ljubljana at the Department of Experimental Oncology. Her main research interest is *in vitro* and *in vivo* preclinical oncology focused on delivery of drug and genes to the cells and tumors with electrochemotherapy and gene electrotransfer.

Monika Savarin is a Ph.D. in Basic Medical Sciences, and since 2012 employed at the Department of Experimental Oncology, Institute of Oncology Ljubljana. Currently, her main focus is on her Post Doc project, combining radiotherapy and gene therapy for modulating tumor blood vessels. She is also involved in other preclinical studies, focusing on electroporation, immunohistology and vascular targeting genes.

Natasa Kejzar, Ph.D. in Statistics, is employed at the Institute for Biostatistics and Medical Informatics, Faculty of Medicine, University of Ljubljana as an assistant professor and researcher. Her research is in biostatistical methodology, more precisely in clustering, classification and measures of explained variation for different statistical models

Gregor Sersa graduated from the Biotechnical Faculty at theUniversity of Ljubljana in 19 78, where he is currently a professor of molecular biology. He is employed at the Institute of Oncology in Ljubljana as a head of the Department of Experimental Oncology. His specific field of interest is the effect of the electric field on tumor cells and tumors as drug and gene delivery system in different therapeutic approaches. Besides experimental work, he is actively involved in the education of undergraduate and postgraduate students at the University of Ljubljana.

Darja Pavlin graduated from Veterinary faculty at University of Ljubljana in 2000 and obtained her PhD in the field of gene therapy of canine tumors. At the moment she is employed at Clinic for companion animals at Veterinary faculty Ljubljana as an assistant professor, involved in clinical work, research and as a lecturer in different undergraduate programs.

Simona Kranjc, Ph.D. in Basic Medical Sciences, is employed at the Department of Experimental Oncology, Institute of Oncology Ljubljana since 1998. Her main interest of research is preclinical oncology, *in vitro* and *in vivo*. Precisely, she is experienced in research of tumor biology, radiotherapy, electrochemotherapy, gene electrotransfer with different antiangiogenic and immunomodulatory targets, three-dimensional cultures, testing of new drugs and investigating of new gene and drug delivery methods.